

RESEARCH ARTICLE

Differential effects of early growth conditions on colour-producing nanostructures revealed through small angle X-ray scattering and electron microscopy

Katarzyna Janas^{1,*}, Anna Łatkiewicz², Andrew Parnell³, Dorota Lutyk¹, Julia Barczyk¹, Matthew D. Shawkey⁴, Lars Gustafsson⁵, Mariusz Cichoń¹ and Szymon M. Drobnik^{1,6}


ABSTRACT

The costs associated with the production and maintenance of colour patches is thought to maintain their honesty. Although considerable research on sexual selection has focused on structurally coloured plumage ornaments, the proximate mechanisms of their potential condition dependence, and thus their honesty, is rarely addressed, particularly in an experimental context. Blue tit (*Cyanistes caeruleus*) nestlings have ultraviolet (UV)–blue structurally coloured tail feathers, providing a unique opportunity for investigation of the causes of variation in their colour. Here, we examined the influence of early growing conditions on the reflectance and structural properties of UV–blue-coloured tail feathers of blue tit nestlings. We applied a two-stage brood size manipulation to determine which stage of development more strongly impacts the quality of tail feather colouration and microstructure. We used small-angle X-ray scattering (SAXS) and electron microscopy to characterise the nanoscale and microscale structure of tail feather barbs. Nestlings from the broods enlarged at a later stage of growth showed a sex-specific rectrix development delay, with males being more sensitive to this manipulation. Contrary to predictions, treatment affected neither the quality of the barbs' nanostructures nor the brightness and UV chroma of feathers. However, at the microscale, barbs' keratin characteristics were impaired in late-enlarged broods. Our results suggest that nanostructure quality, which determines the UV–blue colour in tail feathers, is not sensitive to early rearing conditions. Furthermore, availability of resources during feather growth seems to impact the quality of feather microstructure more than body condition, which is likely to be determined at an earlier stage of nestling growth.

KEY WORDS: Blue tit, Early-rearing conditions, Microstructure, Rectrices, Small angle X-ray scattering, Structural colouration

¹Institute of Environmental Sciences, Jagiellonian University, Gronostajowa 7, 30-387 Kraków, Poland. ²Institute of Geological Sciences, Jagiellonian University, Gronostajowa 3a, 30-387 Kraków, Poland. ³Department of Physics and Astronomy, The University of Sheffield, The Hicks Building, Sheffield S3 7RH, UK. ⁴Evolution and Optics of Nanostructures, Department of Biology, University of Ghent, K. L. Ledeganckstraat 35, 9000 Gent, Belgium. ⁵Department of Animal Ecology/Ecology and Genetics, Uppsala University, Norbyvägen 18 D, 752 36 Uppsala, Sweden. ⁶School of Biological, Environmental and Earth Sciences, University of New South Wales, Kensington Sydney, NSW 2052, Australia.

*Author for correspondence (k.janas@doctoral.uj.edu.pl)

 K.J., 0000-0002-0646-2543; A.Ł., 0000-0001-6206-6476; A.P., 0000-0001-7956-7939; D.L., 0000-0003-0878-2767; M.D.S., 0000-0002-5131-8209; L.G., 0000-0001-6566-2863; M.C., 0000-0002-6164-6951; S.M.D., 0000-0001-8101-6247

Received 6 May 2020; Accepted 28 July 2020

INTRODUCTION

Birds are among the most vividly coloured animals, with conspicuous plumage produced by wavelength-specific absorption of pigments deposited in the feathers, by interaction of light with nanometre-scale structures inside feather barbs or barbules, or by a combination of these two mechanisms (Prum et al., 1998; Prum, 2006; Stavenga et al., 2011; Tinbergen et al., 2013; Shawkey and D'Alba, 2017). Avian colouration can have numerous functions, from concealment via cryptic plumage or mimicry to advertising the quality of an individual (reviewed in Bortolotti, 2006). In this lattermost context, colour displays may function as signals in mate choice, competition between individuals of the same sex, or parent–offspring communication. However, an important prerequisite of such signalling is signal honesty, which prevents cheating by lower-quality individuals. According to the condition capture models, the honesty of the signals in the colour patches is ensured by the costs associated with its production and/or maintenance (Zahavi, 1977; Grafen, 1990). This implies that only individuals in the best condition are able to express and bear the highest-quality colour ornaments. In the case of sexually selected traits, another prediction that stems from those models is heightened condition dependence of colour ornaments in males (reviewed in Cotton et al., 2004).

Despite being built on a firm theoretical framework (Pomiankowski, 1987; Grafen, 1990), empirical support from well-designed experiments for the condition-dependence model of colour ornaments is still very scarce (Cotton et al., 2004). One notable exception is carotenoid-based colouration, which is unusual in that it cannot be synthesised *de novo* by birds (McGraw, 2006a,b).

The under-representation of studies investigating condition dependence is especially striking in the case of structurally coloured ornaments, which – being particularly visually conspicuous – are often the subject of research on sexual selection. Leaving aside white, achromatic feathers (where the colour is produced by even scattering of all wavelengths), bright structural colours are generated by coherent light scattering by keratin nanostructures and melanosomes (Prum et al., 1998; Prum, 2006; Wilts et al., 2014; Igic et al., 2016). Such colouration can be divided into iridescent colouration, generated by laminar or crystal-like nanostructures located in the feather barbules, and matte, non-iridescent colouration produced by quasi-ordered spongy-like keratin nanostructures inside the barbs (Prum and Torres, 2003). The honesty of structurally coloured ornaments is thought to be ensured by the costs of keratin and melanin pigment production (Meadows et al., 2012). However, earlier histological studies suggested that the growth of spongy nanostructure involves few to no metabolic costs (Shawkey et al., 2006; Prum et al., 2009). To our knowledge, there are no experimental studies examining the proximate mechanisms of condition dependence of nanostructures, and only a few previous studies addressing relationships between



Fig. 1. Eighteen-day-old blue tit (*Cyanistes caeruleus*) nestlings inside the nest box.

structure and colour variation in general: for iridescent colour in the satin bowerbird (*Ptilonorhynchus violaceus*; Doucet et al., 2006), and for non-iridescent colour in the bluebird (*Sialia sialis*; Shawkey et al., 2003, 2005), the blue tit (*Cyanistes caeruleus*; Hegyi et al., 2018) and nine species of fairywren (*Malurus* spp.; Fan et al., 2019).

The timing of physiological impacts on feather colour and quality are also unstudied. Some evidence comes from studies on feather renewal processes. The quality of feathers is sensitive to perturbations or stressors during moult in adult birds (e.g. Griggio et al., 2009; Vágási et al., 2012), and juvenile feathers produced during energetically demanding periods of nestling growth are even more sensitive to early rearing conditions (Tschirren et al., 2003; Jacot and Kempenaers, 2007). During the first days of a nestling's life, the majority of nutrients are invested in rapid growth and intensive metabolic processes, but also in feather follicle formation. After the feather pins are visible, the internal barb cells continue to mature, so processes important for the development of colour-producing structures occur while the feather is growing (Prum et al., 2009). Thus, the question of how early growing conditions affect the structural coloration of juvenile feathers can be complemented with a further question: which stage of a nestling's growth is most important in this process.

Here, we used an experimental brood size manipulation to investigate the influence of early rearing conditions on non-

iridescent structural colouration of blue tit nestlings. The blue tit is a widespread cavity nester that readily breeds in nest boxes, simplifying the monitoring of nestlings. More importantly, it has contrasting, conspicuous plumage. These features make it a particularly suitable model species for studying colouration in birds. Experimental studies are facilitated by the fact that juvenile blue tits express ultraviolet (UV)-blue, non-iridescent structural colouration in the tail feathers (Fig. 1), with greater expression levels in males (Johnsen et al., 2003). Furthermore, in contrast to the breast feathers, which are replaced during the post-juvenile moult, most tail feathers are moulted only after the first breeding season, which means that they may play a signalling function in parent-offspring communication and – beyond the nestling period – in mate choice. Consequently, variation in this particular ornamented trait could be subjected to different selection pressures (Jacot and Kempenaers, 2007). Both breast and tail colouration of blue tit nestlings were shown to be condition dependent in correlational (Johnsen et al., 2003) and experimental (Jacot and Kempenaers, 2007) studies, but only the latter study showed a sex-specific effect on rectrices structural colouration. A recent quantitative genetics study, besides finding low heritability of tail structural colouration, surprisingly showed that, at a genetic level, UV chroma of rectrices is negatively related to the proxies of a bird's performance: body mass, wing length and cell-mediated immunity (Class et al., 2019).

In this study, we used a two-stage brood size manipulation design, with nests enlarged either at an early or late stage of nestlings' growth. Brood size manipulation has repeatedly been shown to affect nestlings' traits, including body mass, tarsus length, condition, immune response and colouration (e.g. Cichoń and Dubiec, 2005; Jacot and Kempenaers, 2007). Here, as a criterion for dividing the development of chicks into two phases, we determined that pins of tail feathers begin to appear on the skin surface around the sixth day after hatching. Among the early-enlarged nests, one group was reduced back to the original brood size in the second stage of nestlings' growth, whereas the other remained enlarged. This experimental design allows us to discriminate at which stage of nestlings' growth greater within-nest competition more strongly influences the developing plumage. We predicted that impaired early-growth conditions should negatively influence barbs' microscale morphology and thus their brightness and UV chroma. We predicted that this effect would be stronger in nestlings from early-enlarged broods, compared with the late-enlarged and control broods. Furthermore, given the sex-specific condition dependence of tail feather colouration found by Jacot and Kempenaers (2007),

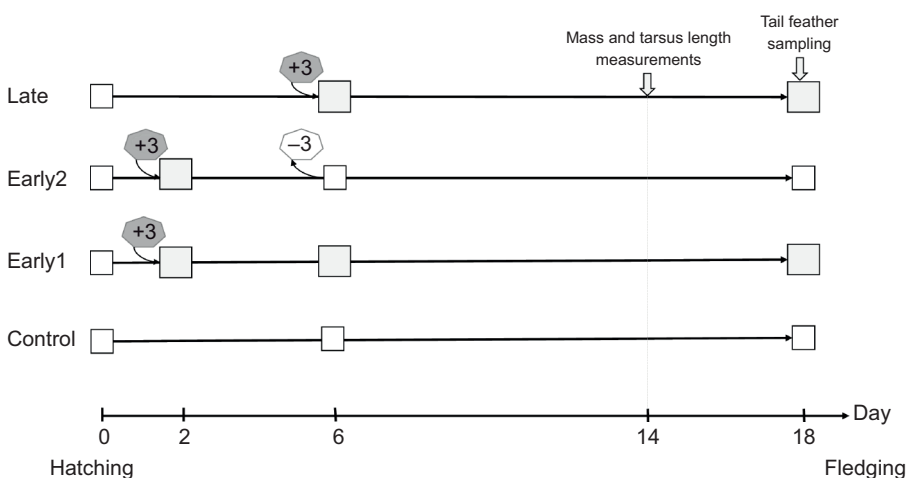


Fig. 2. The experimental design scheme for two-stage *C. caeruleus* brood size manipulation.

Bigger, light grey squares indicate nests with broods enlarged by three nestlings; smaller, white squares denote nests with broods that were not manipulated or broods that were restored to their initial size. Dark grey and white heptagons indicate, respectively, the procedure of brood size enlargement and reduction.

we predicted that the internal structure of male feathers would be significantly different from that of female feathers, and more sensitive to deterioration of early-development conditions.

MATERIALS AND METHODS

Field study

The study was conducted over two field seasons: 2017 and 2018, in a nest-box population of blue tits [*Cyanistes caeruleus* (Linnaeus 1758)], inhabiting the island of Gotland (Sweden, 57°01'N 18°16' E). The study area is covered with fields and meadows, having patches of deciduous and mixed forests, dominated by oak (*Quercus robur*) and ash (*Fraxinus excelsior*), with an admixture of hawthorn (*Crataegus* spp.) and hazel (*Corylus avellana*) (for more detailed description, see Pärt and Gustafsson, 1989). In this population, hatching date can vary between mid-May and the beginning of June, the incubation period lasts 2 weeks, and the majority of nestlings from one nest hatch during a single day, although some degree of hatching asynchrony is observed. Nestlings are fed mainly with caterpillars, less often with mosquitos or spiders, and fledge 18–22 days after hatching (Drobniak et al., 2014).

From the end of April, we regularly inspected nest boxes to track the nest-building process, and assess the number of eggs and the beginning of the incubation period. During the incubation, females were not disturbed until the expected hatching date. On the second day after hatching, we weighed nestlings, marked them by nail clipping and took a small blood sample from the tarsal vein. On the eighth day after hatching, we ringed the nestlings, and on the 14th day, we weighed and measured the tarsus length of nestlings. On day 18, we collected the second right rectrix from each nestling. We regressed the body mass at day 14 against the tarsus length to obtain a measure of mass, independent of body size. Further, in this paper, we refer to the measure as 'residual mass' (in other studies this metric is also called body condition, e.g. in Jacot and Kempnaers, 2007).

Experimental protocol and sampling

To manipulate nestlings' rearing conditions we performed a two-stage brood size manipulation experiment, with three types of enlarged broods (Fig. 2). In the 'Early1' group, the brood size was enlarged at day 2 and left without further manipulation until fledging. The second group, 'Early2', was enlarged at day 2, but donor nestlings were removed at day 6 and transferred to nests from the third group, 'Late'. The fourth group was not manipulated and constituted a 'Control'. Nests for the experiment were chosen to create blocks of four nests with matched hatching date (± 1 day) and number of nestlings (± 1 egg), plus one donor nest (not considered in further analyses) with the same hatching date. Both Early1 and Early2 groups were enlarged by three randomly chosen chicks from the donor nest. At day 6, when donor nestlings from the Early2 group were relocated to the Late group, we also visited the nests from the remaining groups, to keep the disturbance level equal. We had six experimental blocks with a total of 214 nestlings in the first breeding season and five blocks in the following season, with 206 nestlings in total (see Table S1 for exact numbers of nestlings in each experimental group).

Feather morphology and colouration

We measured the total length of plucked tail feather samples (distance from feather tip to the end of the calamus) and the length of the feather sheath of rectrices with a digital calliper to the nearest 0.1 mm. To estimate the degree of feather development, we divided the length of the erupted part of the feather by the total feather length (hereafter referred to as 'development coefficient').

Feather reflectance measurements were performed using an Ocean Optics Maya Flame spectrophotometer (Dunedin, FL, USA) with bifurcated probe 7×400 μm and a xenon pulsed light source. On each rectrix, we made 10 reflectance measurements along the outer (the most brightly coloured) vane. Obtained spectra were averaged, smoothed and further analysed using the package pavo (Maia et al., 2013) in R (version 3.1.2). For spectral analysis we calculated a set of reflectance-based colour metrics, among which we chose brightness (total reflectance), UV chroma and red chroma for further analysis, with UV chroma and red chroma calculated, respectively, as the sum of reflectance values of regions from 300 nm to 400 nm and from 605 nm to 700 nm, divided by the total reflectance in the given region (Maia et al., 2013).

Molecular sex assessment

DNA was extracted from blood samples stored in 96% ethanol, using Chelex (Bio-Rad, Munich, Germany) following the manufacturer's protocol (Walsh et al., 1991). Sexing was performed following a well-established PCR-based method (Griffiths et al., 1998).

Scanning electron microscopy (SEM)

To compare the internal microstructure morphology of the feather barbs we used SEM. The order of the nests for SEM preparations was generated randomly, and from each experimental nest we randomly chose (by drawing envelopes with samples) three nestlings for SEM rectrix preparations. Donor nestlings (in groups Early1 and Late) and feathers with erupted parts shorter than 1 cm were excluded from the analysis. After removing 2–3 mm of the distal tip of a feather, a fragment of the rectrix outer vane was sliced perpendicularly to the barbs, so that the cut-out fragment contained 6–11 barb cross-sections. The sectioned fragment was mounted on a graphite block covered with carbon adhesive tape and sputter coated with gold. Samples were viewed on a HITACHI S-4700 cold-field-emission scanning electron microscope at $\times 1300$ and $\times 5000$ magnifications. From each feather, three cross-sections were chosen, excluding the outermost feather, the one closest to the vane, as well as the ones that were crushed, damaged or contaminated by visible debris. Using ImageJ software (<https://imagej.nih.gov/ij/>), we measured the following characteristics of the barb's microstructure (Fig. 3B): height and width of a cross-section, number and area of air cavities, the area of the medullary part, the cortex area, the total area, total number of melanosomes and melanosome density (D'Alba et al., 2014).

Small-angle X-ray scattering (SAXS)

In many previous studies (since the early work of Dyck, 1971), feather nanostructures were analysed with transmission electron microscopy, which gives very precise, high-quality images. However, owing to the time-consuming preparation and the probability of sample shrinkage this method has some limitation in quantitative studies on bigger sample sizes (Saranathan et al., 2012). Instead, we used SAXS to quantitatively characterise the length scales of the nanostructures present in the barbs (Saranathan et al., 2012; Parnell et al., 2015). SAXS analysis allows us to predict the interaction between the incident light and the nanostructure of the analysed sample, and therefore predict the optical properties of the feather (Saranathan et al., 2012). In subsequent analysis, we used the following metrics: maximum peak height, peak position and full-width at half-maximum of the peak (further referred to as FWHM). Maximum peak height relates to the intensity of the scattering of nanostructures, and SAXS peak position (in the

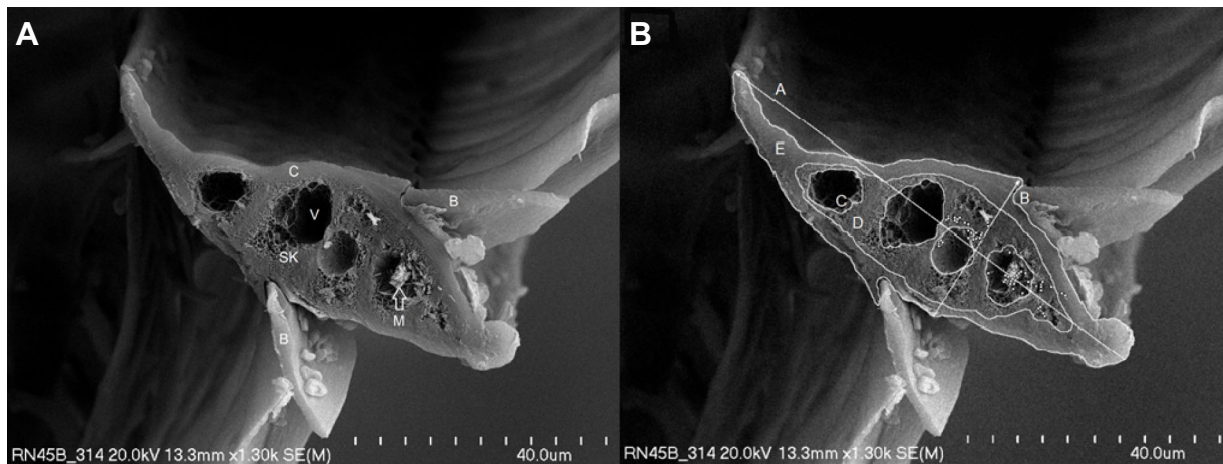


Fig. 3. Characteristics of the barb microstructure in *C. caeruleus*. (A) SEM image of barb cross-section, showing solid keratin cortex (C), spongy keratin nanostructure (SK), air vacuoles (V), melanosomes (M) and barbules (B). (B) Parameters measured in the ImageJ software: height (A), width (B), area of air cavities (C), medullary area (D), total area (E) and melanosomes (marked with white dots).

q domain) is inversely proportional to the wavelength position of the peak reflectance. The FWHM value is a measure of the nanostructure size distribution (short-range quasi-periodic order). Narrow structural peaks with a smaller FWHM mean more defined nanostructure, while higher values of FWHM indicate a larger spread in length scales, and thus a broader optical reflectance peak, meaning less saturated colours (Saranathan et al., 2012).

The SAXS measurements were performed on a subset of tail feathers from the 2017 season. We excluded samples from donor nestlings and underdeveloped or poor-quality feather samples, which eventually resulted in a sample size of 166 individuals, with equal numbers in experimental groups ($\chi^2=0.48$, d.f.=3, $P=0.92$). SAXS measurements were carried out using a Xeuss 2.0 (Xenocs, Grenoble, France) SAXS system, with a liquid gallium X-ray source (MetalJet Excillum, Sweden). The feather samples were mounted in an aluminium frame and the measurements were taken from the region of the outer vane, located 5 mm below the distal tip of the feather. The X-ray beam (9.24 keV) diameter was 300 μm vertically and 250 μm horizontally, with a distance of 6.5 m between sample and detector (Pilatus3R 1M 2D, Dectris, Switzerland). Each individual feather sample was measured for a period of 180 s, with the data being processed using the software Foxtrot 3.3 (Soleil, France); the detector images were masked to account for the detector gridlines and hot pixels, and the image was then radially integrated to give the scattered intensity as a function of the scattering wave vector q (Saranathan et al., 2012). The structural peak from the optical nanostructure in the feathers was measured using the SAXS scattering curve transformed into the Lorentz corrected Iq^2 versus q form, and the structural peak was fitted using a Lorentz peak function.

Statistical analysis

The overall sample size, after excluding all donor nestlings, comprised 420 birds, from 44 experimental nests (Table S1), equally distributed between experimental groups ($\chi^2=0.057$, d.f.=3, $P=0.996$). Owing to nestlings fledging before sampling of tail feathers (two whole nests in 2018 and numerous individual cases) or inadequate quality of collected samples, the sample size for feather colouration was reduced to 334. The sex was assigned for 375 nestlings, with equal sex ratio, confirmed by a Chi-square test ($\chi^2=0.45$, d.f.=1, $P=0.502$).

To test for differences in the survival rate between experimental groups, a generalised linear mixed model with a binomial error was applied, with fledging success introduced as the dependent variable, experimental group as a fixed factor and nest as a random term. The effects of experimental treatment on nestlings' residual body mass, tarsus length, tail feather development, colouration, microstructure and nanostructure characteristics were analysed using a general linear mixed effect model. The models included experimental treatment, nestling sex and year as fixed explanatory variables, and nest of rearing defined as a random term. In all analyses, we first tested for the interaction between experimental treatment and sex of the nestlings, but wherever this interaction was not significant it was removed from the models.

Because some of the characteristics obtained from SEM images might be interdependent, a principal component analysis (PCA) was used to summarise barb microstructure variables. We extracted the first two principal components (PCs), explaining 59.95% and 18.43% of variance, respectively, which were used as dependent variables in further analysis (see Fig. 6 for a biplot of PC1 and PC2). PC1 had very strong negative loadings for total area of cross-section (-0.97) and area of medullary part (-0.96), medium negative loadings for the rest of the keratin-based variables (Table S2), and medium (-0.63) and low (-0.25) loading, respectively, for the number and density of melanosomes. Thus, PC1 described the size and internal structure of barbules, with higher values of PC1 signifying thinner, flatter barbules with less cortex and medullary keratin. PC2 described mainly variation in melanin-based component with negative-factor loading for number and density of melanosomes (-0.76 and -0.95 ; Table S2). Thus, PC2 could be interpreted as a melanosome scarcity parameter: higher values indicating lower numbers of melanosomes. The first two PCs were further used as dependent variables in subsequent analysis. In those two models, to account for potential differences between the cross-section resulting from the distance from the rachis, the numbered order of a cross-section was introduced as an additional explanatory variable in the analysis. Because we analysed three cross-sections per individual, the individual identity was introduced as another random term. All analyses were performed in R using the lme4 and lmerTest packages for linear mixed models, factoextra for PCA analysis and ggplot2 for graphs (<http://www.R-project.org/>).

Table 1. Experimental data on *Cyanistes caeruleus* nestling mass, tarsus length, tail feather morphometrics and colour metrics, tail feather barb cross-section microstructure variables and small angle X-ray scattering (SAXS) metrics

A	Control (N=105)	Early1 (N=106)	Early2 (N=106)	Late (N=103)
Mass	10.97±1.20	10.96±1.16	10.99±1.16	10.96±1.16
Tarsus	16.79±0.63	16.79±0.62	16.78±0.63	16.79±0.62
Rectrix length	32.17±4.18	31.96±4.16	31.82±4.23	31.85±4.17
Rectrix sheath	14.18±1.62	13.98±1.72	14.05±1.70	13.99±1.74
Erupted part	18.03±4.07	18.00±4.06	17.80±4.07	17.88±4.10
Tail brightness*	4605.21±667.89	4629.18±687.27	4582.23±673.12	4596.28±686.02
Tail UV chroma*	0.28±0.02	0.28±0.02	0.28±0.02	0.28±0.02
B	Control (N=33)	Early1 (N=25)	Early2 (N=32)	Late (N=30)
Height	64.685±11.307	65.358±11.334	65.167±11.623	65.550±12.163
Width	18.230±2.577	18.236±2.592	18.256±2.621	18.205±2.712
Total area	799.794±245.509	808.132±246.539	810.049±253.004	814.791±267.615
Medullary area	427.099±154.541	433.938±157.207	432.882±160.976	439.850±167.999
Cortex area	376.453±113.696	378.494±112.001	381.833±114.929	379.889±121.004
Vacuoles	4.4±1.4	4.4±1.4	4.5±1.4	4.5±1.4
Vacuole area	167.505±76.570	167.169±74.361	166.205±74.920	170.068±76.637
Melanosomes	90.078±64.745	93.128±67.997	94.766±68.189	98.272±69.313
Melanosomes per area	0.113±0.070	0.114±0.071	0.117±0.072	0.120±0.071
C	Control (N=42)	Early1 (N=40)	Early2 (N=36)	Late (N=40)
Maximum peak height	1.01E-11±3.80E-12	1.06E-11±4.02E-12	9.92E-12±3.60E-12	1.04E-11±3.77E-12
Peak position	3.01E-03±1.85E-04	3.03E-03±1.89E-04	3.01E-03±1.89E-04	3.02E-03±1.87E-04
Peak FWHM	3.20E-03±3.02E-04	3.23E-03±3.01E-04	3.20E-03±2.95E-04	3.25E-03±3.08E-04

(A) Nestling mass, tarsus length, tail feather morphometrics and colour metrics. (B) Tail feather barb cross-section microstructure variables. (C) SAXS metrics. Means±s.d. are shown. *Sample size for colour metric measurements: Control, N=80; Early1, N=76; Early2, N=82; Late, N=101. FWHM, full-width at half-maximum of the peak.

RESULTS

Nestling body mass, tarsus length and fledging success

The mean±s.d. values of nestling mass, tarsus length, tail feather parameters and colour metrics, averaged within experimental group and sex are provided in Table 1A and Table S4A, respectively. At day 14, experimental treatment affected nestlings' residual body mass negatively in the Early1 group and positively in the Early2 group (Table 2). Tarsus length was not affected by experimental manipulation in any of the groups (Table 2). For both residual mass and tarsus length, the interaction between experimental treatment and nestling sex was not significant in any of the groups. There was no difference in nestlings' fledging success between the experimental groups (Early1: estimate±s.e.: -1.40±1.06, $P=0.18$; Early2: estimate±s.e.: 0.07±1.12, $P=0.95$; Late: estimate±s.e.: 0.86±1.17, $P=0.46$) and the average fledging success was 87.17%.

Tail feather development and colouration

Tail feathers were significantly shorter in chicks of enlarged broods, and this effect was more marked among males (Table 2, Fig. 4C). This pattern was even stronger for the rectrix coefficient of development, where interaction with sex appeared significant also in the Early2 group, with the same effect direction (Table 2). Contrary to predictions, colour metrics of tail feathers were not significantly affected by experimental manipulation (Table 3, Table S3). However, there was a close-to-significant trend of lower UV chroma in the Late group. Independently of experimental manipulation, UV chroma was significantly higher in males (Table 3, Fig. 5A), whereas red chroma was higher in females (Table S3).

Micro- and nanostructural characteristics of tail feathers

SEM images of barbs' rami cross-sections revealed a medullary area consisting of dead keratinocytes containing channel-type β -keratin spongy nanostructure with interspersed melanosomes and centrally located air cavities (Fig. 4A, Fig. S1). Nestlings from late-enlarged

broods had smaller diameters of barbs' keratin morphological elements (PC1; Table 4, Fig. S2A), while other groups did not differ from the control. Number and density of melanosomes (PC2) did not differ between groups (Table 4, Fig. S2B). In both models with PCs, there were differences between sexes, with males having wider and thicker barbs, larger medullary area and more air vacuoles, and tending to have more melanosomes, relative to female chicks (Table 4). The means±s.d. of tail feather barb cross-section microstructure variables, averaged within experimental group or sex, are provided in Table 1B and Table S4B, respectively.

None of the quantitative SAXS metrics (maximum peak height, peak position, FWHM) were affected by experimental manipulation (Table 5); however, for the FWHM, the estimate in the Late group was an order of magnitude higher than in both early-enlarged groups. The interaction between experimental treatment and sex of the nestlings was not significant in any of the models, although there were significant differences in all three SAXS metrics between males and females (Fig. 5B,C). This means that male keratin nanostructures generate shorter-wavelength reflectance peaks (according to the position of the SAXS peak in q space), have stronger scattering keratin nanostructures (according to the intensity of the SAXS scattering) and – most importantly – are characterised by more regular structure than female keratin nanostructures (according to the FWHM parameter) (Table 5). The means±s.d. of the tail feather SAXS metrics, averaged within experimental group or sex, are provided in Table 1C and Table S4C, respectively.

DISCUSSION

The experimental treatment significantly affected residual body mass in both of the early-enlarged groups; however, only in the group that remained enlarged was the effect negative as predicted (Table 2, Fig. 3A). Nestlings from the Early2 group, with broods enlarged only during the first days of early growth, unexpectedly turned out to be heavier, and this effect was consistent for both

Table 2. Results of the linear mixed models, showing the effects of experimental double-stage brood size manipulation on *C. caeruleus* nestlings' residual mass, tarsus length and development of tail feathers

	Estimate	s.e.	d.f.	t	P
Residual mass					
Intercept	959.606	317.040	37.270	3.027	0.004**
Exp. group (Early1)	-0.592	0.220	36.453	-2.695	0.011*
Exp. group (Early2)	0.620	0.227	37.122	2.735	0.010**
Exp. group (Late)	-0.111	0.220	36.328	-0.507	0.615
Sex (male)	0.080	0.064	326.759	1.247	0.213
Year (2018)	-0.476	0.157	37.269	-3.027	0.004**
Tarsus length					
Intercept	-359.151	312.465	36.686	-1.149	0.258
Exp. group (Early1)	-0.305	0.217	36.315	-1.404	0.169
Exp. group (Early2)	-0.027	0.224	36.757	-0.121	0.904
Exp. group (Late)	0.011	0.217	36.270	0.051	0.960
Sex (male)	0.441	0.041	320.401	10.722	<0.001***
Year (2018)	0.186	0.155	36.685	1.203	0.237
Rectrix length					
Intercept	-3682.806	2272.514	36.632	-1.621	0.114
Exp. group (Early1)	-1.441	1.636	38.911	-0.881	0.384
Exp. group (Early2)	2.608	1.594	39.073	1.636	0.110
Exp. group (Late)	1.118	1.586	38.378	0.705	0.485
Sex (male)	1.734	0.503	277.039	3.448	<0.001***
Year (2018)	1.841	1.126	36.632	1.634	0.111
Exp. group (Early1): sex (male)	-0.522	0.764	277.776	-0.683	0.495
Exp. group (Early2): sex (male)	-1.068	0.745	278.773	-1.433	0.153
Exp. group (Late): sex (male)	-2.095	0.714	277.575	-2.935	0.004**
Erupted part					
Intercept	-4180.363	2238.893	34.091	-1.867	0.071
Exp. group (Early1)	-1.028	1.625	39.528	-0.633	0.531
Exp. group (Early2)	1.870	1.583	39.665	1.181	0.245
Exp. group (Late)	0.934	1.574	38.866	0.594	0.556
Sex (male)	1.035	0.559	276.369	1.851	0.065
Year (2018)	2.081	1.110	34.090	1.875	0.069
Exp. group (Early1): sex (male)	-0.485	0.846	277.314	-0.573	0.567
Exp. group (Early2): sex (male)	-1.413	0.825	278.476	-1.712	0.088
Exp. group (Late): sex (male)	-2.629	0.791	277.086	-3.323	0.001**
Rectrix coefficient					
Intercept	-75.919	42.454	32.647	-1.788	0.083
Exp. group (Early1)	0.013	0.031	41.803	0.408	0.686
Exp. group (Early2)	0.037	0.031	41.768	1.191	0.240
Exp. group (Late)	0.035	0.030	40.738	1.149	0.257
Sex (male)	0.023	0.013	279.388	1.757	0.080
Year (2018)	0.038	0.021	32.646	1.801	0.081
Exp. group (Early1): sex (male)	-0.026	0.020	280.739	-1.282	0.201
Exp. group (Early2): sex (male)	-0.044	0.020	282.234	-2.220	0.027*
Exp. group (Late): sex (male)	-0.070	0.019	280.502	-3.670	<0.001***

The model included experimental (exp.) group, year and sex as fixed factors and the nest of rearing as a random term. Reference levels for fixed effects: exp. group, Control; sex, female; year, 2017. * $P < 0.05$, ** $P < 0.01$, *** $P < 0.001$.

experimental seasons. Late enlargement of the brood did not change nestlings' body mass. However, interestingly, in this group we observed a sex-specific rectrix development delay, with males being more sensitive to the experimental manipulation than females (Table 2, Fig. 3C). An analogous pattern, but with smaller effect size, was present in the Early2 group. Therefore, the effect of the experimental manipulation on the parameters connected with general condition was different for each of the experimental groups.

Contrary to predictions, neither brightness nor UV chroma of tail feathers was affected in any of the experimental groups. The only detectable tendency was a non-significant decrease in UV chroma in the Late group, with an estimated similar order of magnitude as the increase in UV chroma in males relative to females. Accordingly, in Jacot and Kempenaers (2007), a study with brood size manipulation, blue tit nestlings from enlarged nests did not differ

from the controls with regard to brightness and UV chroma of tail feathers. However, males raised in reduced broods developed feathers with higher UV chroma. This sex-specific effect was hypothesised to be the result of early-acting sexual selection, as tail feathers are not replaced during post-juvenile moult, and this was hypothesised to play a signalling role in mate choice during the first breeding season (Jacot and Kempenaers, 2007; Class et al., 2019; Badás et al., 2020). Interestingly, in a brood size manipulation experiment on eastern bluebirds (*Sialia sialis*), structurally coloured wing feathers were also shown to be brighter in male nestlings from reduced broods, compared with those from enlarged broods, whereas no analogous effect was found in females (Siefferman and Hill, 2007). In accordance with our results, manipulation of early-rearing conditions did not change feathers' UV chroma, although in both cases it was significantly higher in males than in females. It seems important that in the above published studies,

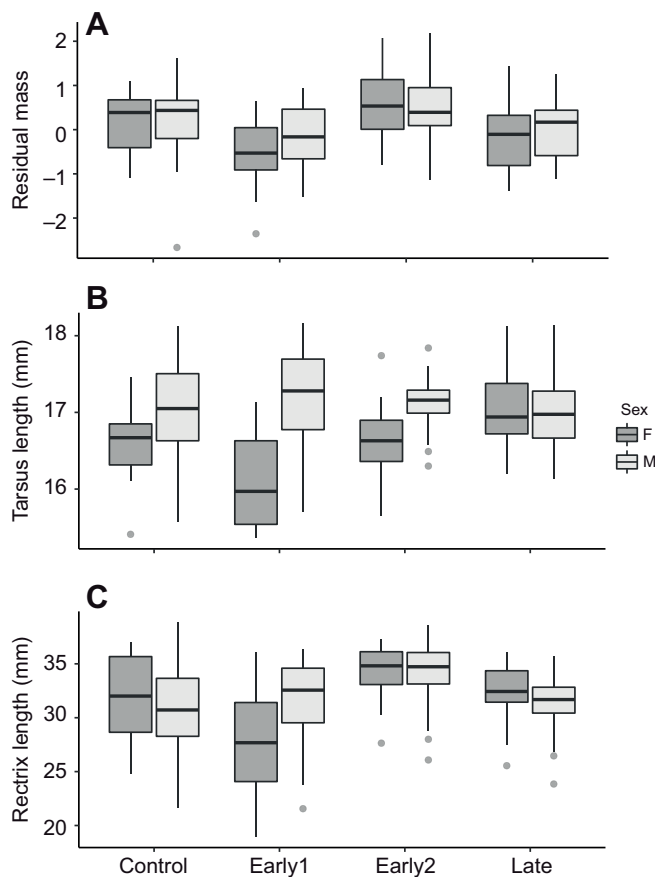


Fig. 4. Differences in residual mass, tarsus length and rectrix length among *C. caeruleus* experimental groups. (A–C) Measures of residual mass (A), tarsus length (B) and rectrix length (C) are shown for Control, Early1, Early2 and Late groups. In the Early1 group, broods were enlarged at day 2 and left without further manipulation until fledging; in the Early2 group, broods were enlarged at day 2 and subsequently reduced at day 6; in the Late group, broods were enlarged at day 6; and in the Control group, broods were not manipulated. Black horizontal bars indicate the median, whiskers indicate minimum and maximum values, and dark-grey and light-grey colours denote, respectively, females and males. Control, $N=105$; Early1, $N=106$; Early2, $N=106$; Late, $N=103$.

observed effects appeared for males in reduced broods, i.e. in improved early-growing conditions, whereas brood size enlargement did not produce a symmetrical negative effect. It is possible that in our study the colour difference was obscured by the difficulty of accurately measuring the colour of very thin and narrow outer vanes of freshly developed nestling rectrices. Thus, we have tried to explore possible underlying colour moderators, looking at the nano- and microscale characteristics of the assayed feathers.

In non-iridescent UV–blue feather colour, hue and UV chroma, in particular, depend on the arrangement of nanoscale keratin structures in the medullary part of the feather barb (Prum, 1998, Shawkey et al., 2005). We found significant sex differences, with males having higher values of all three SAXS metrics (Fig. 5B,C). Most importantly, males exhibited higher q -value-centred peaks, which indicates smaller short-range quasi-periodic order of nanostructure (Saranathan et al., 2012) and hence shorter wavelength of peak reflectance (shifted towards UV), which explains dichromatism in UV chroma. These results emphasise that the SAXS method detects patterns complementary to spectrophotometric predictions, even in relatively thin, finely coloured and freshly developed feathers such as those used in our study. Nevertheless, contrary to predictions, we found no differences in the SAXS morphometrics between experimental groups. Perhaps this low sensitivity of spongy structure to manipulated early-growing conditions might be explained by the likelihood that nanostructures in the medullary cells are produced via self-assembly in a process called spinodal decomposition, which does not require significant energy input or limiting nutrients (Prum et al., 2009).

However, other microstructural elements of barb morphology and their characteristics are also critical to the mechanism of colour production (Fan et al., 2019). At the microscale, we found that barb characteristics were impaired in late-enlarged broods. Width of barb cross-section, total area, medullary area, vacuole number and area all decreased, but the density of melanosomes was not affected (although we noted a very-close-to-significant trend of lower melanosome numbers in the Late group; Table 4). This is only a partial confirmation of our expectations, because we predicted an analogous, but more strongly pronounced, effect in both early-enlarged groups. We must note that SEM imaging is not an optimal

Table 3. Results of the linear mixed models, showing effects of experimental double-stage brood size manipulation on *C. caeruleus* nestlings' tail feather colour metrics

	Estimate	s.e.	d.f.	t	P
Brightness					
Intercept	586,303.900	317,823.780	35.420	1.845	0.074
Exp. group (Early1)	34.340	222.260	35.490	0.155	0.878
Exp. group (Early2)	−132.230	217.350	35.950	−0.608	0.547
Exp. group (Late)	−97.610	213.620	33.960	−0.457	0.651
Sex (male)	−78.510	68.390	273.470	−1.148	0.252
Year (2018)	−288.290	157.540	35.420	−1.830	0.076
UV chroma					
Intercept	5.592	8.554	32.680	0.654	0.518
Exp. group (Early1)	0.001	0.006	32.710	0.139	0.890
Exp. group (Early2)	−0.001	0.006	33.140	−0.090	0.929
Exp. group (Late)	−0.009	0.006	31.300	−1.544	0.133
Sex (male)	0.015	0.002	271.300	8.120	<0.001***
Year (2018)	−0.003	0.004	32.680	−0.622	0.538

The model included experimental (exp.) group and sex as fixed factors and the nest of rearing as a random term. Reference levels for fixed effects: exp. group, Control; sex, female; year, 2017. *** $P<0.001$.

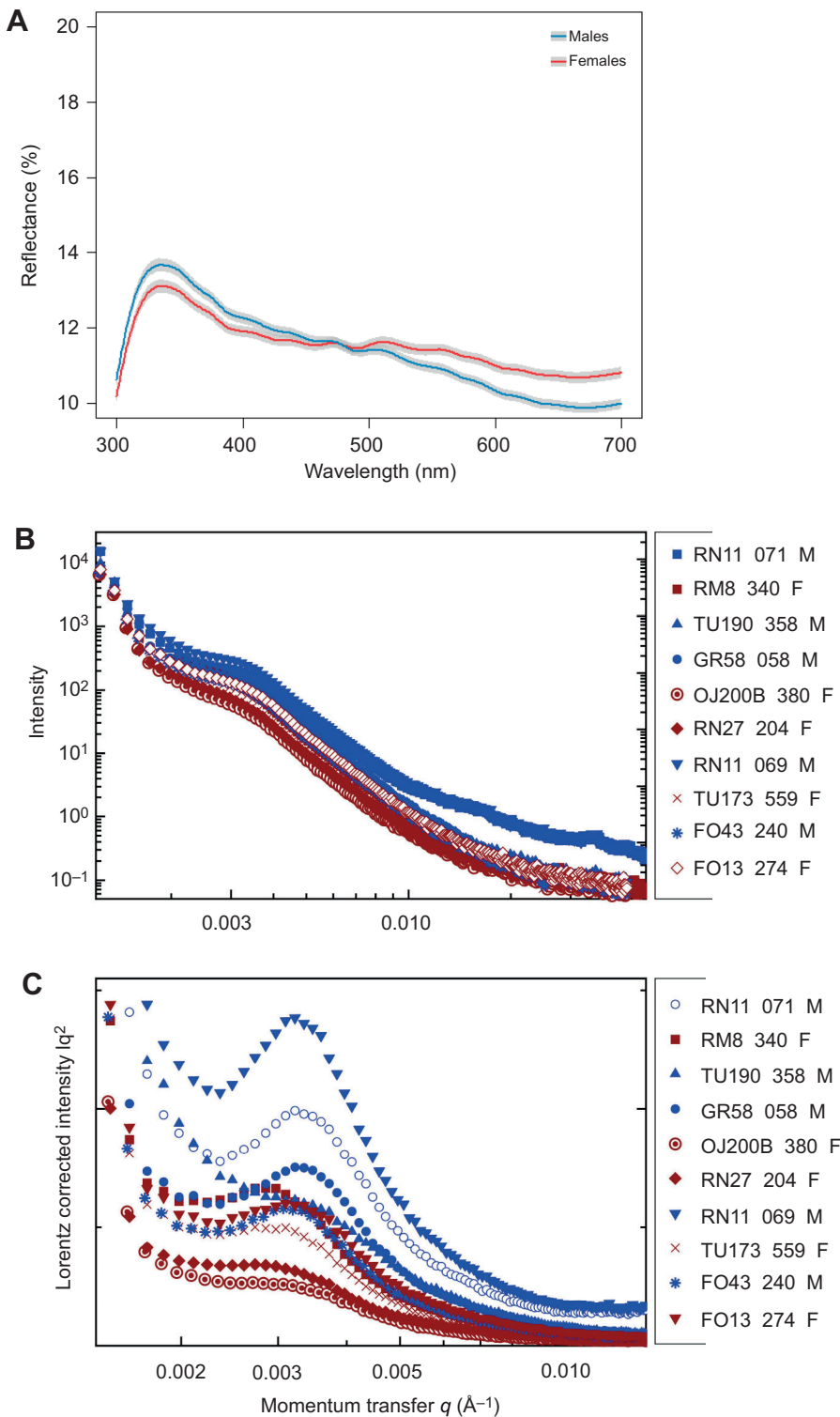


Fig. 5. Reflectance spectra and small-angle X-ray scattering (SAXS) data of *C. caeruleus* nestlings' tail feather outer vane. (A) Averaged reflectance spectra of blue tit nestlings' tail feather outer vane. Blue and red lines indicate, respectively, male and female mean reflectance; grey shading indicates s.e. The sample size was 141 and 164 for females and males, respectively. (B,C) Example SAXS data (B) and Lorentz corrected SAXS data (C) curves of blue tit nestlings' tail feather outer vane, of 10 randomly chosen individuals. Males and females are indicated with blue and brown, respectively. Alphanumeric codes represent individual nest boxes and the three last digits are the nestlings' ring numbers.

method for measuring melanosome density (owing to low contrast, making discrimination between morphological features difficult), and we treat this parameter more as an approximation than an exact value. However, the pattern we obtained for the Late group shows some similarity to that obtained by D'Alba et al. (2014), examining condition dependence of melanin-based colouration in zebra finches (*Taeniopygia guttata*) exposed to unpredictable food supply during development and black-capped chickadees (*Poecile atricapillus*) affected by avian keratin disorder. In both cases, the density of

melanosomes did not differ between control and experimental groups, while barbule density (keratin component) was consistently higher in controls (D'Alba et al., 2014). This can be explained by the fact that melanin is endogenously synthesised (McGraw, 2006a, b), and currently there is no evidence that would indicate that it is expensive to produce.

We predicted that the negative effect of impaired early-growth conditions on feather structure and colouration would be more pronounced in nestlings from early-enlarged broods, compared with

Table 4. Results of the linear mixed models, showing effects of experimental double-stage brood size manipulation on *C. caeruleus* tail feather barb cross-section microstructure characteristics, expressed as principal components

	Estimate	s.e.	d.f.	t	P
PC1					
Intercept	-1890.000	1057.000	34.710	-1.788	0.083
Exp. group (Early1)	1.119	0.739	37.520	1.514	0.138
Exp. group (Early2)	0.564	0.713	36.760	0.791	0.434
Exp. group (Late)	1.823	0.708	35.830	2.576	0.014*
Sex (male)	-1.269	0.349	101.200	-3.634	<0.001***
Year (2018)	0.938	0.524	34.710	1.790	0.082
Cross-section	-0.371	0.031	240.500	-11.803	<0.001***
PC2					
Intercept	-882.484	478.699	35.331	-1.844	0.074
Exp. group (Early1)	-0.443	0.333	34.745	-1.331	0.192
Exp. group (Early2)	-0.450	0.321	34.185	-1.404	0.169
Exp. group (Late)	-0.539	0.316	32.712	-1.704	0.098
Sex (male)	-0.479	0.196	106.236	-2.448	0.016*
Year (2018)	0.438	0.237	35.334	1.847	0.073
Cross-section	-0.184	0.034	286.622	-5.351	<0.001***

Reference levels for fixed effects: exp. group, Control; sex, female; year, 2017; cross-section, -2. * $P < 0.05$, *** $P < 0.001$.

late-enlarged and control broods. However, in terms of feather development and microstructure, the most sensitive to manipulation was the Late group. This suggests that the current availability of resources has a greater effect on feather development than current body condition, which could be determined at an earlier stage of nestling growth. Previous experimental studies, with accelerated moult rate in adult birds, demonstrated that feather quality is sensitive to perturbations during feather development (e.g. Griggio et al., 2009, Vágási et al., 2012). However, it is also possible that the smaller barb diameters were caused by the slowdown of tail feather development, as feathers from this group were also shown to be shorter. Our sampling (18th day) took place before the completion of the bottom feather portion growth; thus, we have no data on the final achieved tail feather length. Unfortunately, sampling of young birds in the period between fledging and the next breeding season is virtually impossible.

We predicted that feather structure would differ between males and females, and that males would be more sensitive to the manipulation of early growing conditions. Indeed, sex differences

were present at all levels of feather structure: from the length of rectrices, through the microscale parameters of barbs, to the nanoscale characteristics, described by SAXS metrics. However, feather colour did not vary in relation to brood enlargement. Within the optical properties, we found that beside the UV region, with reflectance higher in males, significant differences are also present at long wavelengths, except that in this region higher reflectance occurs in females. According to Fan et al. (2019), reflectance at long wavelengths might depend on the spatial frequency and thickness of spongy layer and cortex. Perhaps then, higher reflectance in the long-wavelength region in females results from the larger nanostructure of the spongy structures in females' feathers (as suggested by the larger values of both SAXS peak position and FWHM in females; Saranathan et al., 2012). To a certain extent, reflectance at long wavelengths might also be affected by the density of melanosomes, which is higher in males. However, absorption properties of melanin decline with increasing wavelength (Xiao et al., 2018); therefore, this factor might have only a limited effect.

Table 5. Results of the linear mixed models, showing effects of experimental double-stage brood size manipulation on *C. caeruleus* tail feather nanostructure SAXS metrics

	Estimate	s.e.	d.f.	t	P
Maximum peak height ¹					
Intercept	1.076	0.143	18.953	7.545	4.02E-07***
Exp. group (Early1)	-0.240	0.208	17.617	-1.156	0.263
Exp. group (Early2)	-0.002	0.209	18.096	-0.012	0.991
Exp. group (Late)	-0.270	0.199	17.846	-1.357	0.192
Sex (male)	0.097	0.038	126.777	2.537	0.012*
Peak position					
Intercept	2.90E-03	4.84E-05	2.33E+01	59.975	<2E-16***
Exp. group (Early1)	2.80E-06	6.65E-05	1.74E+01	0.042	0.967
Exp. group (Early2)	6.00E-05	6.82E-05	1.87E+01	0.88	0.39
Exp. group (Late)	-2.32E-05	6.42E-05	1.81E+01	-0.361	0.722
Sex (male)	2.06E-04	2.57E-05	1.33E+02	8.033	4.58E-13***
Peak FWHM					
Intercept	3.10E-03	8.34E-05	2.24E+01	37.131	<2E-16***
Exp. group (Early1)	3.87E-05	1.14E-04	1.62E+01	0.340	0.738
Exp. group (Early2)	-4.62E-05	1.17E-04	1.74E+01	-0.395	0.697
Exp. group (Late)	1.30E-04	1.10E-04	1.69E+01	1.186	0.252
Sex (male)	9.88E-05	4.65E-05	1.33E+02	2.126	0.035*

The model included experimental (exp.) group and sex as fixed factors and the nest of rearing as a random term. Reference levels for fixed effects: exp. group, Control; sex, female. ¹Coded variable. FWHM, full-width at half-maximum of the peak. * $P < 0.05$, *** $P < 0.001$.

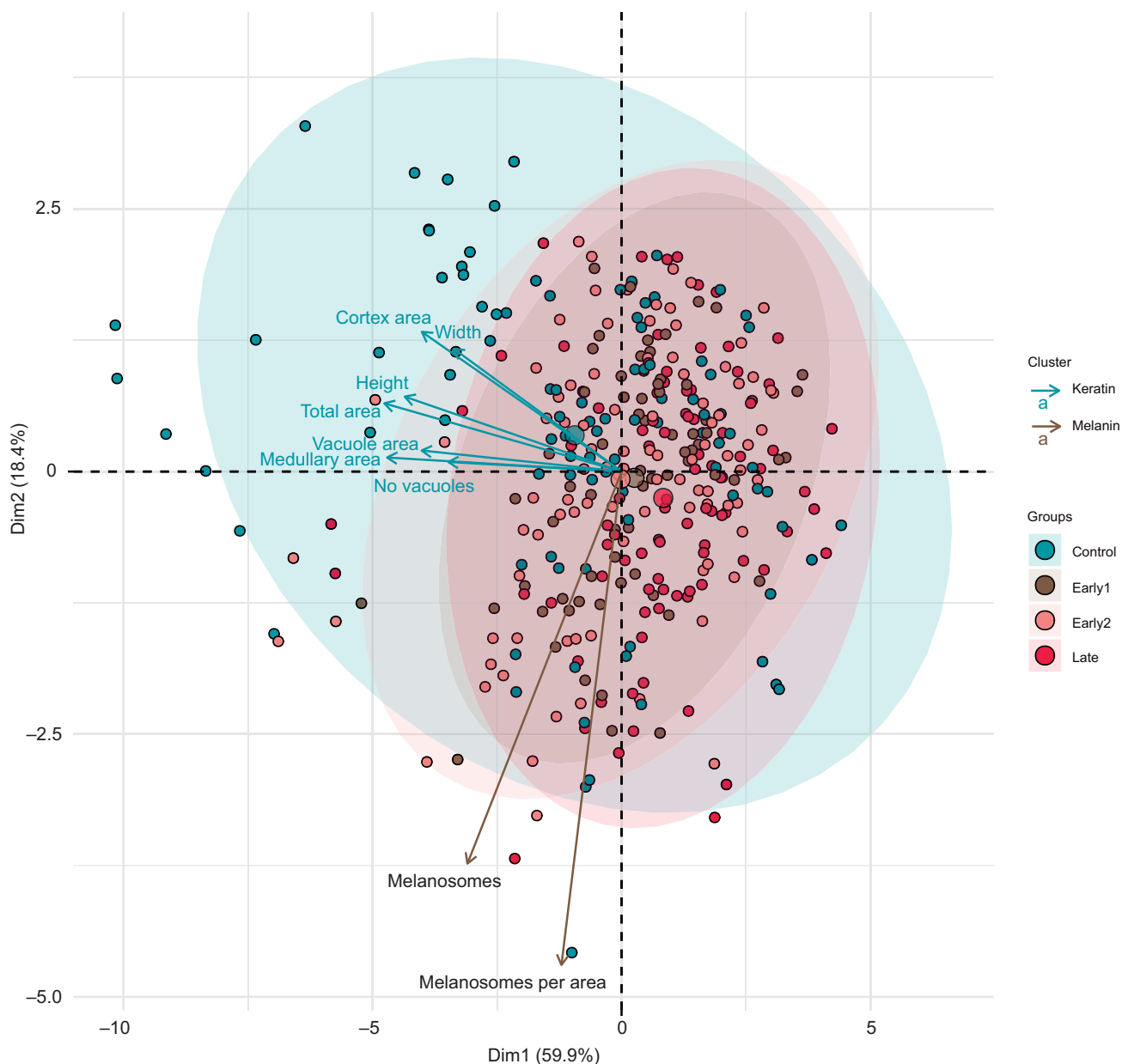


Fig. 6. Principal component analysis biplot of 352 nestlings' tail feathers barb cross-sections. Microscale characteristics are shown as variables, explained by the two principal component axes, categorised as either keratin or melanin cluster and divided into four experimental groups.

Finally, nestlings from the Early2 group (in which broods were enlarged during the first days of development but reduced at day 6) had higher residual body mass, consistently in both of the study seasons. This unexpected result suggests that the amount of parental investment might be fixed at a very early stage of offspring development. Alternatively, the first stage of nestling development might be less costly for parents; however, in this scenario, the negative effect would be of similar strength in the Late group as in Early1, but this was not the case. We suggest a potential future study with similar experimental design, but controlling for parental effort (feeding frequency, quality of food brought to nest) is needed.

To conclude, our results suggest that, contrary to carotenoid-based colouration [which in tits was proposed to be largely determined by the amount of carotenoids deposited to egg yolk and the feeding during the first 6 days (Fitze et al., 2003)], feathers with structural colouration are more sensitive to conditions experienced during

feather growth in the later phases of nesting period. We demonstrated that the quality of the spongy β -keratin nanostructure in the blue tit tail feathers' barbs does not appear to be sensitive to early rearing conditions. However, other keratin components of barb morphology, like the medullary layer area in a barb or the number of air vacuoles, seem to be more sensitive to perturbation during early development. To our knowledge, this is the first experimental study in which SAXS and SEM analysis were applied to quantitatively examine the quality of structural colouration, and the first study that looked at inter-sexual differences in these parameters. Future studies should focus on elucidating the mechanism mediating condition dependence and sexual dichromatism in structurally coloured ornaments.

Acknowledgements

We are thankful to two anonymous reviewers for their constructive comments and suggestions. We are very grateful to Marek Michalik for consent to carry out the SEM

analysis in the Laboratory of Scanning Microscopy, Institute of Geological Sciences, Jagiellonian University, and to Olga Woźnicka and Grzegorz Tylko for introducing K.J. to electron microscopy. We are very grateful to Liliana D'Alba, Bram Vanthournout and other members of the Evolution and Optics of Nanostructures Group, University of Ghent, and Agnieszka Gudowska of the Institute of Environmental Sciences, Jagiellonian University, for helpful and constructive comments on a previous version of the manuscript. We thank Johan Träff for providing photographs of nestlings, as well as Magda Zagalska-Neubauer and Tomasz Kowalczyk for their assistance in the fieldwork.

Competing interests

The authors declare no competing or financial interests.

Author contributions

Conceptualization: K.J., M.D.S., M.C., S.M.D.; Methodology: K.J., A.P., M.D.S., S.M.D.; Software: K.J.; Validation: S.M.D.; Formal analysis: K.J., S.M.D.; Investigation: K.J., A.L., A.P., D.L., J.B., S.M.D.; Resources: K.J., A.L., A.P., L.G., S.M.D.; Data curation: K.J., A.P., S.M.D.; Writing - original draft: K.J.; Writing - review & editing: A.L., A.P., D.L., J.B., M.D.S., L.G., M.C., S.M.D.; Visualization: K.J., A.P.; Supervision: M.C., S.M.D.; Project administration: K.J.; Funding acquisition: K.J., M.D.S., S.M.D.

Funding

This study was financed by Narodowe Centrum Nauki [UMO-2015/19/N/NZ8/00404 to K.J.; UMO-2015/18/E/NZ8/00505 to S.M.D.] and by Fonds Wetenschappelijk Onderzoek [G007117N to M.D.S.].

Data availability

Data sets used in quantitative analyses are available from the figshare data repository: <https://doi.org/10.6084/m9.figshare.12732971.v1>

Supplementary information

Supplementary information available online at <https://jeb.biologists.org/lookup/doi/10.1242/jeb.228387.supplemental>

References

- Badás, E., Autor, A., Martínez, J., Rivero-de Aguilar, J. and Merino, S.** (2020). Individual quality and extra-pair paternity in the blue tit: sexy males bear the costs. *Evolution*, **74**, 559-572. doi:10.1111/evo.13925
- Bortolotti, G. R.** (2006). Natural selection and avian coloration: protection, concealment, advertisement or deception? Chapter 1. In *Bird Coloration: Volume 2: Function and Evolution* (ed. G. E. Hill and K. J. McGraw), pp. 3-35. Harvard University Press.
- Cichoń, M. and Dubiec, A.** (2005). Cell-mediated immunity predicts the probability of local recruitment in nestling blue tits. *J. Evol. Biol.* **18**, 962-966. doi:10.1111/j.1420-9101.2005.00910.x
- Class, B., Kluehn, E. and Brommer, J. E.** (2019). Tail colour signals performance in blue tit nestlings. *J. Evol. Biol.* **32**, 913-920. doi:10.1111/jeb.13489
- Cotton, S., Fowler, K. and Pomiankowski, A.** (2004). Do sexual ornaments demonstrate heightened condition-dependent expression as predicted by the handicap hypothesis? *Proc. R. Soc. Lond. B* **271**, 771-783. doi:10.1098/rspb.2004.2688
- D'Alba, L., Van Hemert, C., Spencer, K. A., Heidinger, B. J., Gill, L., Evans, N. P., Monaghan, P., Handel, C. M. and Shawkey, M. D.** (2014). Melanin-based color of plumage: role of condition and of feathers' microstructure. *Integr. Comp. Biol.* **54**, 633-644. doi:10.1093/icb/ucu094
- Doucet, S. M., Shawkey, M. D., Hill, G. E. and Montgomerie, R.** (2006). Iridescent plumage in satin bowerbirds: structure, mechanisms and nanostructural predictors of individual variation in colour. *J. Exp. Biol.* **209**, 380-390. doi:10.1242/jeb.01988
- Drobnik, S. M., Dubiec, A., Gustafsson, L. and Cichoń, M.** (2014). Maternal age-related depletion of offspring genetic variance in immune response to phytohaemagglutinin in the blue tit (*Cyanistes caeruleus*). *Evol. Biol.* **42**, 88-98. doi:10.1007/s11692-014-9301-8
- Dyck, J.** (1971). Structure and spectral reflectance of green and blue feathers of the rose-faced lovebird (*Agapornis roseicollis*). - Dansk. Vid. Selsk. Biol. Skr. **18**, 1-67.
- Fan, M., D'Alba, L., Shawkey, M. D., Peters, A. and Delhey, K.** (2019). Multiple components of feather microstructure contribute to structural plumage colour diversity in fairy-wrens. *Biol. J. Linn. Soc.* **128**, 550-568. doi:10.1093/biolin/lnz114
- Fitze, P. S., Tschirren, B. and Richner, H.** (2003). Carotenoid-based colour expression is determined early in nestling life. *Oecologia* **137**, 148-152. doi:10.1007/s00442-003-1323-3
- Grafen, A.** (1990). Biological signals as handicaps. *J. Theor. Biol.* **144**, 517-546. doi:10.1016/S0022-5193(05)80088-8
- Griffiths, R., Double, M., Orr, K. and Dawson, R.** (1998). A DNA test to sex most birds. *Mol. Ecol.* **7**, 1071-1075. doi:10.1046/j.1365-294x.1998.00389.x
- Griggio, M., Serra, L., Licheri, D., Campomori, C. and Pilastro, A.** (2009). Molt speed affects structural feather ornaments in the blue tit. *J. Evol. Biol.* **22**, 782-792. doi:10.1111/j.1420-9101.2009.01700.x
- Hegyi, G., Laczi, M., Kötél, D., Cszimadia, T., Lów, P., Rosivall, B., Szöllösi, E. and Török, J.** (2018). Reflectance variation in the blue tit crown in relation to feather structure. *J. Exp. Biol.* **221**, jeb176727. doi:10.1242/jeb.176727
- Igic, B., D'Alba, L. and Shawkey, M. D.** (2016). Manakins can produce iridescent and bright feather colours without melanosomes. *J. Exp. Biol.* **219**, 1851-1859. doi:10.1242/jeb.137182
- Jacot, A. and Kempnaers, B.** (2007). Effects of nestling condition on UV plumage traits in blue tits: an experimental approach. *Behav. Ecol.* **18**, 34-40. doi:10.1093/beheco/arl054
- Johnsen, A., Delhey, K., Andersson, S. and Kempnaers, B.** (2003). Plumage colour in nestling blue tits: sexual dichromatism, condition dependence and genetic effects. *Proc. R. Soc. Lond. B Biol. Sci.* **270**, 1263-1270. doi:10.1098/rspb.2003.2375
- Maia, R., Eliason, C. M., Bitton, P.-P., Doucet, S. M. and Shawkey, M. D.** (2013). pavo: an R Package for the analysis, visualization and organization of spectral data. *Method. Ecol. Evol.* **4**, 906-913. doi:10.1111/2041-210X.12069
- McGraw, K. J.** (2006a). Mechanics of carotenoid-based coloration. Chapter 5. In *Bird Coloration: Volume 1: Mechanisms and Measurements* (ed. G. E. Hill and K. J. McGraw), pp. 177-242. Harvard University Press.
- McGraw, K. J.** (2006b). Mechanics of melanin-based coloration. Chapter 6. In *Bird Coloration: Volume 1: Mechanisms and Measurements* (ed. G. E. Hill and K. J. McGraw), pp. 243-294. Harvard University Press.
- Meadows, M. G., Roudybush, T. E. and McGraw, K. J.** (2012). Dietary protein level affects iridescent coloration in Anna's hummingbirds, *Calypte anna*. *J. Exp. Biol.* **215**, 2742-2750. doi:10.1242/jeb.069351
- Parnell, A. J., Washington, A. L., Mykhaylyk, O. O., Hill, C. J., Bianco, A., Burg, S. L., Dennison, A. J. C., Snape, M., Cadby, A. J., Smith, A. et al.** (2015). Spatially modulated structural colour in bird feathers. *Sci. Rep.* **5**, 18317. doi:10.1038/srep18317
- Pärt, Y., Gustafsson, L.** (1989). Breeding dispersal in the Collared Flycatcher (*Ficedula albicollis*): possible causes and reproductive consequences. *J. Anim. Ecol.* **58**, 305-320. doi:10.2307/5002
- Pomiankowski, A.** (1987). Sexual selection: the handicap principle does work—sometimes. *Proc. R. Soc. Lond. B* **231**, 123-145. doi:10.1098/rspb.1987.0038
- Prum, R. O.** (2006). Anatomy, physics and evolution of structural colors. Chapter 7. In *Bird Coloration: Volume 1: Mechanisms and Measurements* (ed. G. E. Hill and K. J. McGraw), pp. 295-353. Harvard University Press.
- Prum, R. O. and Torres, R. H.** (2003). A Fourier tool for the analysis of coherent light scattering by bio-optical nanostructures. *Integr. Comp. Biol.* **43**, 591-602. doi:10.1093/icb/43.4.591
- Prum, R. O., Torres, R. H., Williamson, S. and Dyck, J.** (1998). Coherent light scattering by blue feather barbs. *Nature* **396**, 28-29. doi:10.1038/23838
- Prum, R. O., Dufresne, E. R., Quinn, T. and Waters, K.** (2009). Development of colour producing β -keratin nanostructures in avian feather barbs. *J. R. Soc. Interface* **6**, S253-S265.
- Saranathan, V., Forster, J. D., Noh, H., Liew, S.-F., Mochrie, S. G. J., Cao, H., Dufresne, E. R. and Prum, R. O.** (2012). Structure and optical function of amorphous photonic nanostructures from avian feather barbs: a comparative small angle X-ray scattering (SAXS) analysis of 230 bird species. *J. R. Soc. Interface* **9**, 2563-2580. doi:10.1098/rsif.2012.0191
- Shawkey, M. D. and D'Alba, L.** (2017). Interactions between colour-producing mechanisms and their effects on the intergenerational colour palette. *Philos. Trans. R. Soc. Lond. B* **372**, 20160536. doi:10.1098/rstb.2016.0536
- Shawkey, M. D., Estes, A. M., Siefferman, L. M. and Hill, G. E.** (2003). Nanostructure predicts intraspecific variation in ultraviolet-blue plumage colour. *Proc. R. Soc. Lond. B* **270**, 1455-1460. doi:10.1098/rspb.2003.2390
- Shawkey, M. D., Estes, A. M., Siefferman, L. M. and Hill, G. E.** (2005). The anatomical basis of sexual dichromatism in non-iridescent ultraviolet-blue structural coloration of feathers. *Biol. J. Linn. Soc.* **84**, 259-271. doi:10.1111/j.1095-8312.2005.00428.x
- Shawkey, M. D., Hill, G. E., McGraw, K. J., Hood, W. R. and Huggins, K.** (2006). An experimental test of the contributions and condition dependence of microstructure and carotenoids in yellow plumage coloration. *Proc. R. Soc. B* **273**, 2985-2991. doi:10.1098/rspb.2006.3675
- Siefferman, L. and Hill, G. E.** (2007). The effect of rearing environment on blue structural coloration of eastern bluebirds (*Sialia sialis*). *Behav. Ecol. Sociobiol.* **61**, 1839-1846. doi:10.1007/s00265-007-0416-0
- Stavenga, D. G., Tinbergen, J. H., Leertouwer, L. and Wilts, B. D.** (2011). Kingfisher feathers – colouration by pigments, spongy nanostructures and thin films. *J. Exp. Biol.* **214**, 3960-3967. doi:10.1242/jeb.062620
- Tinbergen, J., Wilts, B. D. and Stavenga, D. G.** (2013). Spectral tuning of Amazon parrot feather coloration by psittacofulvin pigments and spongy structures. *J. Exp. Biol.* **216**, 4358-4364. doi:10.1242/jeb.091561
- Tschirren, B., Fitze, P. S. and Richner, H.** (2003). Sexual dimorphism in susceptibility to parasites and cell-mediated immunity in Great Tit nestlings. *J. Anim. Ecol.* **72**, 839-845. doi:10.1046/j.1365-2656.2003.00755.x
- Vágási, C. I., Pap, P. L., Vincze, O., Benkő, Z., Marton, A. and Barta, Z.** (2012). Haste makes waste but condition matters: molt rate – feather quality trade-off in

- a sedentary songbird. *PLoS ONE* **7**, e40651. doi:10.1371/journal.pone.0040651
- Walsh, P. S., Metzger, D. A. and Higuchi, R.** (1991). Chelex-100 as a medium for simple extraction of DNA for PCR-based typing from forensic material. *BioTechniques* **10**, 506-513.
- Wilts, B. D., Michielsen, K., De Raedt, H. and Stavenga, D. G.** (2014). Sparkling feather reflections of a bird-of-paradise explained by finite-difference time-domain modeling. *Proc. Natl. Acad. Sci. USA* **111**, 4363-4368. doi:10.1073/pnas.1323611111
- Xiao, M., Chen, W., Li, W., Zhao, J., Hong, Y.-I., Nishiyama, Y., Miyoshi, T., Shawkey, M. D. and Dhinojwala, A.** (2018). Elucidation of the hierarchical structure of natural eumelanins. *J. R. Soc. Interface* **15**, 20180045. doi:10.1098/rsif.2018.0045
- Zahavi, A.** (1977). The cost of honesty—(further remarks on handicap principle). *J. Theor. Biol.* **67**, 603-605. doi:10.1016/0022-5193(77)90061-3

Supplementary material

Table S1. Number of nests and individuals in each experimental group in a given breeding season.

	Nests	Nestlings:	Early 1	Early 2	Late	Control	All nestlings
2017	24		54	54	51	55	214
2018	20		52	52	52	50	206
Both Seasons	44		106	106	103	105	420

Table S2. Values of PC loading for variables characterizing microstructure of barb's cross-sections.

Variable	PC1	PC2
height	-0.89	0.14
width	-0.69	0.24
total area	-0.97	0.13
medullary area	-0.96	0.03
cortex area	-0.82	0.27
no. of vacuoles	-0.71	0.02
vacuoles area	-0.82	0.04
melanosomes	-0.63	-0.76
melanosomes density	-0.25	-0.96

Table S3.

Results of the linear mixed models showing effects of experimental double-stage brood size manipulation on red chroma of tail feathers. The model included experimental group, year and sex as fixed factors and nest of rearing as a random term. Reference levels for fixed effects: exp. group – CONTROL; sex – female; year – 2017.

	Estimate	SE	df	t	p
Red chroma					
Intercept	-5.769	4.597	31.880	-1.255	0.219
Early1	0.003	0.003	32.270	0.904	0.372
EarlyY2	0.000	0.003	32.060	0.904	0.935
Late	0.005	0.003	29.680	1.708	0.098
Sex: Males	-0.013	0.001	274.300	-10.262	<0.001 ***
year	0.003	0.001	31.880	1.303	0.202

Table S4. Mean value and standard deviation of **A.** nestlings mass, tarsus length, tail feathers morphometrics and colour metrics (*sample size of colour metrics measurements was 164 and 141 for males and females, respectively), averaged within sex; **B.** tail feather barb cross-section microstructure variables; **C.** small angle X-ray scattering (SAXS) metrics. **B.** Analysis of barbs microstructure characteristics was performed on subsample of 3 randomly chosen nestlings from each experimental nest, therefore the sample size within each sex is given in brackets in column headings. **C.** SAXS analysis was performed on a subset of tail feathers from the 2017 season, thus the sample size within sex is given in brackets in column headings.

A.	Males (n = 222)	Females (n =205)
mass	10.97 ± 1.15	10.97 ± 1.15
tarsus length	16.79 ± 0.62	16.79 ± 0.62
rectrix length	31.87 ± 4.15	31.86 ± 4.15
rectrix sheath	14.00 ± 1.74	13.99 ± 1.73
erupted part	17.89 ± 4.08	17.89 ± 4.08
tail brightness*	4608.13 ± 686.36	4608.14 ± 686.35
Tail UV chroma*	0.28 ± 0.02	0.28 ± 0.02
B.	Males (n = 69)	Females (n = 46)
Height	65.24 ± 11.56	65.12 ± 11.42
Width	18.23 ± 2.64	18.19 ± 2.60
Total area	808.38 ± 252.95	803.45 ± 247.36
Medullary area	433.43 ± 160.57	430.93 ± 157.68
Cortex area	379.17 ± 114.15	376.75 ± 112.02
No vacuoles	4.44 ± 1.39	4.43 ± 1.38
Vacuoles area	167.45 ± 75.02	166.71 ± 74.01
Melanosomes	94.32 ± 68.75	92.72 ± 67.68
Melanosomes per area	0.12 ± 0.07	0.11 ± 0.07
C.	Males (n = 95)	Females (n = 53)
Maximum peak height	9.79E-12 ± 3.67E-12	9.81E-12 ± 3.67E-12
Peak position	3.03E-03 ± 1.95E-04	3.02E-03 ± 1.96E-04
Peak FWHM	3.20E-03 ± 2.97E-04	3.20E-03 ± 2.98E-04

Figures

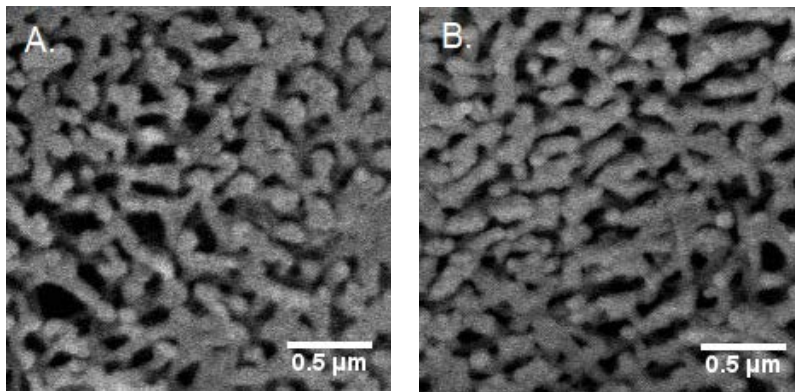


Fig. S1. SEM micrographs of the female (A.) and male (B.) rectrix barb cross-section, showing fragment with keratin spongy structure.

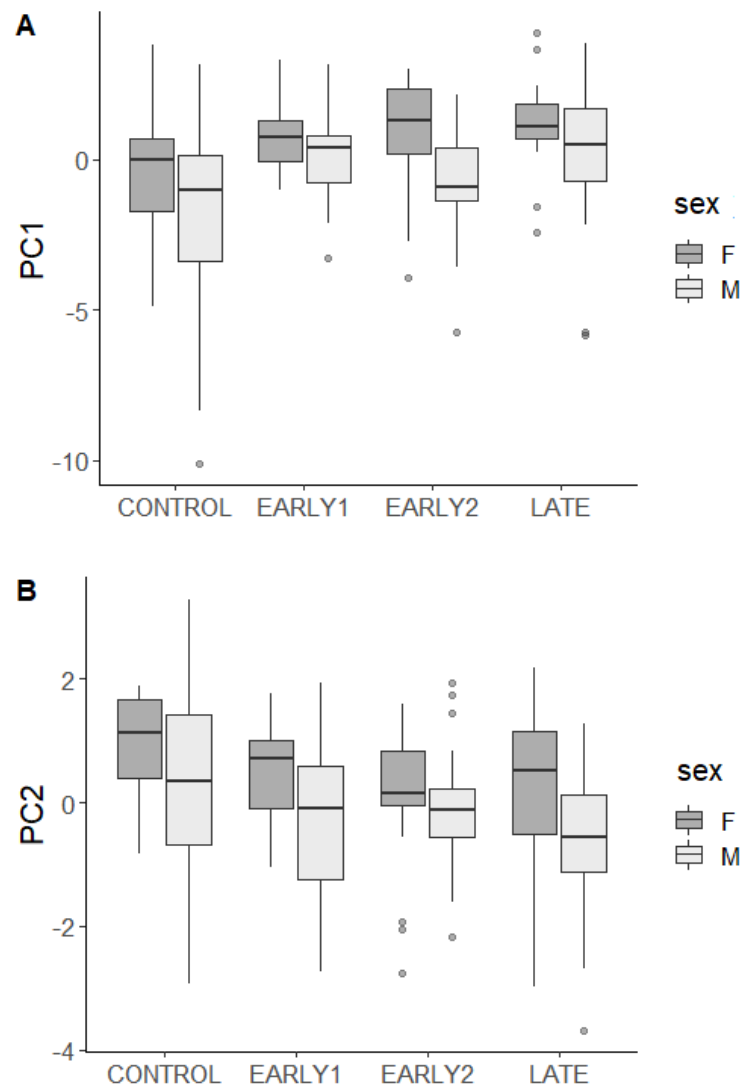


Figure S2. Differences in PC1 (A), and PC2 (B) between experimental groups. “Early1” indicate the group in which broods were enlarged at day 2 and left without further manipulation until fledging, in the group “Early2” broods were enlarged at day 2, and subsequently reduced at day 6, in the group “Late” broods were enlarged at day 6, and “Control” was the group with not manipulated broods. Black horizontal bars indicate median, whiskers indicate minimum and maximum values, dark grey and light grey colours denote, respectively, females and males.